Journal of The Electrochemical Society, **155** (3) A201-A205 (2008)
0013-4651/2008/155(3)/A201/5/$23.00 © The Electrochemical Society

$M_3(PO_4)_2$-Nanoparticle-Coated $LiCoO_2$ vs $LiCo_{0.96}M_{0.04}O_2$ (M = Mg and Zn) on Electrochemical and Storage Characteristics

Junho Eom and Jaephil Cho*,z

Department of Applied Chemistry, Hangyang University, Ansan, Korea 426-791

The electrochemical cycling and storage characteristics of $LiCo_{0.96}M_{0.04}O_2$ and $M_3(PO_4)_2$ nanoparticle-coated $LiCoO_2$ cathode materials (M = Zn and Mg) were compared at room temperature and 90°C between 3 and 4.5 V. The doped cathodes showed degraded electrochemical performance at room temperature compared to the uncoated cathode. The first discharge capacities of the uncoated and the doped cathodes were 186 and 175 mAh/g, respectively. The doped cathodes showed 30 mAh/g after 30 cycles, while the uncoated cathode showed 100 mAh/g after 50 cycles at a 1 C rate. $Mg_3(PO_4)_2$ and $Zn_3(PO_4)_2$-coated $LiCoO_2$ showed discharge capacities of 179 and 187 mAh/g, respectively, and hadsignificantly improved capacity retention, showing 133 and 153 mAh/g, respectively, after 50 cycles. After storage at 90°C, in the electrolytes using 4.5 V charged electrodes, the doped cathodes showed both greatly decreased side reactions with the electrolytes and formation of Co_3O_4 and CoO phases from Li and Co dissolution. However, the coated cathodes did not show either structural transformation into the Co_3O_4 and CoO phases or side reactions with the electrolytes.
 [DOI: 10.1149/1.2827993]

Manuscript submitted May 23, 2007; revised manuscript received October 29, 2007. Available electronically January 8, 2008.

At present, $LiCoO_2$ powders are the most widely used cathode material in Li-ion batteries for mobile electronics, which alter the charge cutoff voltage from 4.2 V (vs graphite) (~4.3 V vs lithium metal) to 4.4 V (vs graphite) (~4.5 V vs lithium metal). By increasing the cutoff voltage, the energy density of the cell can be increased by ~15%. However, due to side reactions with the electrolytes on the particle surface and continuous structural destruction from the dissolution of Li and Co ions, the capacity of $LiCoO_2$ rapidly the fades. Previous studies have focused on improvements of electrochemical performances at room temperature using doped $LiCo_{1-x}M_xO_2$ (M = Al, Zn, Ti, and Mg)[1,2] or coatings.[3-14] Here, coatings may be an attractive method for improving such problems, as it applies only to final $LiCoO_2$ materials. For doped cathodes, depending on the dopants (M) in $LiCo_{1-x}M_xO_2$ and the value of x, the specific capacity varies. In addition, uniform substitution of dopants into the Co 3*b* sites in the $LiCoO_2$ are difficult to achieve in mass-production processes that use solid-state reactions.

Only a small number of storage studies at elevated temperatures (e.g., 90°C) have been reported[15,17] thus far. MPO_4 coatings (M = metal) have been reported to be effective in improving not only thermal stability but also electrochemical properties, depending on the M factor.[15] In a $FePO_4$ coating, Fe ions were observed to be dissolved into the electrolytes during 90°C storage. For an $AlPO_4$ coating, despite improving the structural stability at 90°C, it has been observed that the capacity decreases at a 1C rate as the electrode density increases.[16] Recently, the authors investigated a $Co_3(PO_4)_2$ coating on $LiCoO_2$ and $LiNi_{0.86}Co_{0.1}Al_{0.04}O_2$ cathodes, which resulted in better rate capabilities compared to an $AlPO_4$ coating at higher C rates.[16,17] However, thus far, a systematic comparison of coated and doped cathodes in terms of cycling and structural stability at 90°C has not been reported.

In this study, a comparison of $Mg_3(PO_4)_2$ and $Zn_3(PO_4)_2$ coatings on $LiCoO_2$ vs doped $LiCo_{0.96}M_{0.04}O_2$ (M = Mg and Zn) cathodes is made regarding the electrochemical properties at room temperature and the structural stability when in storage at 90°C after charging at 4.5 V in electrolytes.

Experimental

$LiCoO_2$ was prepared by stoichiometric mixing of Co_3O_4 (99.99%, average particle size 3 μm) and Li_2CO_3 and firing at 1000°C for 3 h. $LiCo_{0.95}M_{0.05}O_2$ (M = Zn and Mg) was prepared by stoichiometric mixing of $Mg(OH)_2$ or ZnO with Co_3O_4 by dry milling at 300 rpm for 48 h. The mixture was then thoroughly mixed with Li_2CO_3 by dry milling at 200 rpm, followed by firing at 600°C for 5 h. The cooled powders were remixed and fired at 1000°C for 3 h. The average particle size of 10 μm uncoated and doped $LiCoO_2$ were used for the electrochemical tests (Brunaner–Emmett–Teller surface area of the samples was 0.5 m^2/g). For scientific accuracy, same uncoated $LiCoO_2$ was used for coatings. Inductively coupled plasma-mass spectroscopy (ICP-MS) results of lithium stoichiometry (x) in the uncoated Li_xCoO_2 showed 1.01. To prepare the coating solution, 3 g of Mg or Zn nitrates and 1.14 g of $(NH_4)_2HPO_4$ were dissolved in 30 g of distilled water, and $M_3(PO_4)_2$ particles that were pink in color instantly precipitated in the solution, which was stirred for 20 min at pH ~4. This coating concentration was a 3 wt % coating concentration (the weight of cathode was fixed at 100 g). For instance, a 1.5 wt % coating concentration was a coating concentration that used 1.5 g of zinc nitrate and 0.57 g of $(NH_4)_2HPO_4$ per 100 g of cathode powders. The coated cathodes were annealed at 800°C for 5 h in air. For the storage test at 90°C, the charged cathodes at 4.5 V were dissembled from coin-type half cells in a glove box and were immersed in electrolyte and tightly sealed in vials. The vials were kept at 90°C for 1 day and cooled to room temperature.

The field-emission transmission electron microscope (FE-TEM) (JEOL 2100F operating at 200 kV) samples were prepared by evaporation of the dispersed particles in acetone or hexane on carbon-coated copper grids. Powder X-ray diffraction (XRD) measurements were carried out using a Rigaku D/Max2000 with a Cu target tube. ICP-MS (ICPS-1000IV, Shimadzu) was used to determine the metal contents. The electrochemical properties were tested in a coin-type 2016R cell with lithium metal as the anode. The cathode consisted of 94 wt % active material, 3 wt % Super P carbon black, and 3 wt % polyvinylidene fluoride binder. The electrolyte for the coin-type half-cells (2016 type) was 1 M $LiPF_6$ with ethylene carbonate/diethylene carbonate/ethyl-methyl carbonate (30:30:40 vol %) (Cheil Ind. Korea). The capacity and capacity retention were measured to be between 3 and 4.5 V at a rate of 0.1, 0.2, 0.5, and 1C (1C = 180 mA/g). Specific capacities of the cathodes were calculated using only the active material. The HF level in the electrolyte solution was determined by gas chromatography.

Results and Discussion

Figure 1 shows XRD patterns of the coated $LiCoO_2$ and doped $LiCo_{0.96}M_{0.04}O_2$ (M = Mg and Zn) powders. Characteristic lines of α-$NaFeO_2$ structure can be observed. Single-phase oxide was ob-

* Electrochemical Society Active Member.
z E-mail: jpcho123@naver.com

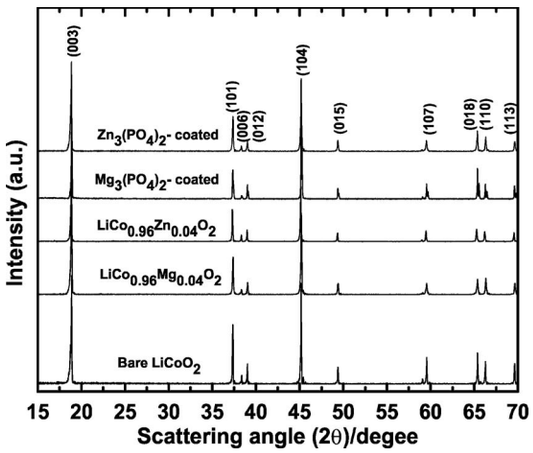

Figure 1. XRD patterns of the $LiCo_{0.96}M_{0.04}O_2$ (M = Zn and Mg) and $Mg_3(PO_4)_2$ and $Zn_3(PO_4)_2$ nanoparticle-coated $LiCoO_2$ powders.

tained, for which Miller indexes (*hkl*) are indexed for a hexagonal setting. For the $LiCo_{0.96}M_{0.04}O_2$ powders, the lattice constants *a* and *c* values increase while those of the coated cathodes are identical to those of uncoated sample, as shown in Table I. The increase in lattice constants in the doped cathodes may be due to the larger size of Mg^{2+} and Zn^{2+} compared with that of the Co^{3+} ions (rMg^{2+} = 0.72 Å), rCo^{3+} = 0.545 Å, rZn^{4+} = 0.74 Å. Figure 2 shows TEM images of the $LiCo_{0.96}M_{0.04}O_2$ (M = Zn and Mg) and the coated samples. The doped samples show typical lattice fringes of the (003) plane corresponding to 4.68 Å. In the case of the $Zn_3(PO_4)_2$-coated sample, its low-magnification image (Fig. 2c) does not show any coating layer, but its high-resolution image (2d) shows an amorphous coating layer with a thickness of ~5 nm. It was found that, depending on the metal (M) in $M_x(PO_4)_2$, the crystallinity and coating thickness varied. For instance, for the $Co_3(PO_4)_2$-coated sample, the $Co_3(PO_4)_2$ coating layer became olivine Li_xCoPO_4 as a result of a reaction with Li in $LiCoO_2$ during the annealing process.[16,17] For the $AlPO_4$ coating, the coating layer was amorphous and its thickness was ~15 to 20 nm.[6] For the $Mg_3(PO_4)_2$-coated sample, nanoparticles <50 nm were coated on the $LiCoO_2$ (Fig. 2e), and the amorphous coating layer that consisted of many pores and rough surfaces with a coating thickness of ~5 nm was also observed (Fig. 2f). In contrast to $Co_3(PO_4)_2$ coating that exhibited the disappearance of the coating layer due to its complete reaction with the bulk surface, $M_3(PO_4)_2$-coated $LiCoO_2$ cathodes (M = Zn and Mg) showed the clearly distinguishable coating layer on the cathode surface, consisting of amorphous phase. Thus, it is believed that $M_3(PO_4)_2$ nanoparticles had a partial reaction of bulk $LiCoO_2$ during an annealing process at 800°C.

Figure 3 shows the charge and discharge curves of the uncoated and doped cathodes for each first cycle at 0.1, 0.2, 0.5, and 1C rates (1C = 180 mA/g) and after 30 or 50 cycles in coin-type half cells. For an uncoated cathode, the first charge and discharge capacities

Table I. XRD lattice constants *a* and *c* and *c*/*a* ratio for $LiCo_{0.96}M_{0.04}O_2$ (M = Zn and Mg) and $Mg_3(PO_4)_2$ and $Zn_3(PO_4)_2$ nanoparticles-coated $LiCoO_2$.

Material	*a* (±0.001 Å)	*c* (±0.001 Å)	*c*/*a*
$LiCoO_2$	2.816	14.034	4.984
$LiCo_{0.96}Zn_{0.04}O_2$	2.819	14.059	4.987
$LiCo_{0.96}Mg_{0.04}O_2$	2.819	14.060	4.988
$Zn_3(PO_4)_2$ coating	2.816	14.034	4.984
$Mg_3(PO_4)_2$ coating	2.816	14.035	4.984

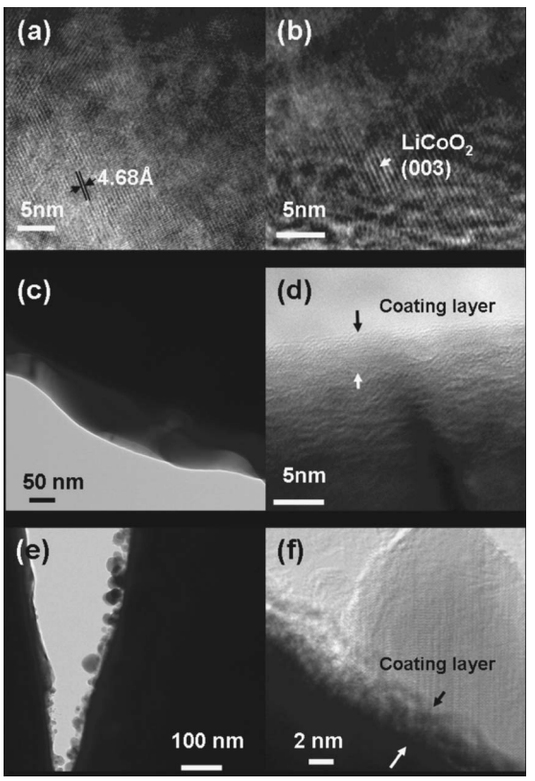

Figure 2. TEM images of the (a) $LiCo_{0.96}Zn_{0.04}O_2$ and (b) $LiCo_{0.96}Mg_{0.04}O_2$ cathode particles (c and d) $Zn_3(PO_4)_2$ nanoparticle-coated $LiCoO_2$ particle [(d) is a magnified image of (c)] and (e and f) $Mg_3(PO_4)_2$ nanoparticle-coated $LiCoO_2$ particle [(f) is a magnified image of (e)].

are 190 and 186 mAh/g, respectively. However, for the Mg-doped cathode, the first charge capacity is similar to that of uncoated cathode at 188 mAh/g, but its discharge capacity decreases to 174 mAh/g. The Zn-doped cathode shows charge and discharge capacities of 188 and 175 mAh/g, respectively. A decrease in the discharge capacities of the doped cathodes is associated with a decrease in the concentration of active Co^{3+} ions and M^{2+} ions substituted into Co sites, leading to the creation of an equal number of Co^{4+} ions for the charge balance. Both $LiCo_{0.96}Zn_{0.04}O_2$ and $LiCo_{0.96}Mg_{0.04}O_2$ exhibit a capacity retention rate of 57% after only 30 cycles, compared with the first discharge capacity at 1C. This retention value is inferior to that of the uncoated cathode with capacity retention of 63% after 50 cycles.

The $Mg_3(PO_4)_2$ and $Zn_3(PO_4)_2$-coated samples (3 wt % coating concentration) show first discharge capacities of 178 and 187 mAh/g, respectively, as shown in Fig. 4. Differential voltage profiles for the uncoated 3, and 1.5 wt % $Mg_3(PO_4)_2$-coated cathodes were added in Fig. 5. The presence of the plateaus between 4 and 4.2 V, indicative of order/disorder phase transition,[18] depends on the coating concentration, and only the 3 wt % coated sample shows the plateau. Our previous study on the $AlPO_4$ coating concentration effect on $LiCoO_2$ also showed a similar result.[19] At this time, we do not know the detailed mechanism for such a phenomenon but doubt it is related to Li stoichiometry difference near the cathode surface. ICP-MS results of lithium stoichiometry (*x*) in the uncoated Li_xCoO_2 showed 1.01. Pereira et al. reported that order–disorder reactions disappeared when the Li stoichiometry (*x*) was $x \approx 1.05$ in Li_xCoO_2.[20] Accordingly, higher $Mg_3(PO_4)_2$ coating concentration may induce the increased difference in Li concentration at the surface and inward, leading to more developed plateaus.

The capacity retention of the $Mg_3(PO_4)_2$ and $Zn_3(PO_4)_2$-coated

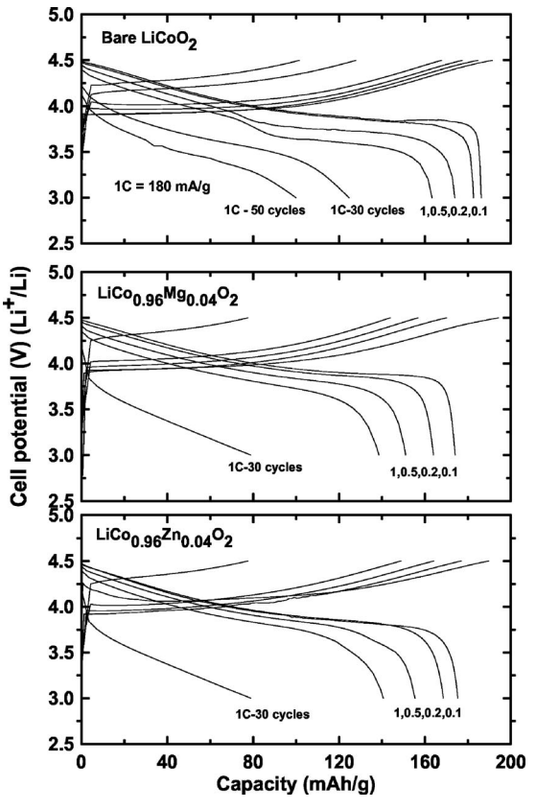

Figure 3. Plots of the cycling curves of coin-type half cells containing uncoated and $LiCo_{0.96}M_{0.04}O_2$ (M = Zn and Mg) cathodes between 3 and 4.5 V at different C rates from 0.1 to 1C (1C = 180 mA/g) and after 30 and 50 cycles at a 1C rate. The same C rates were used during the charge and discharge processes.

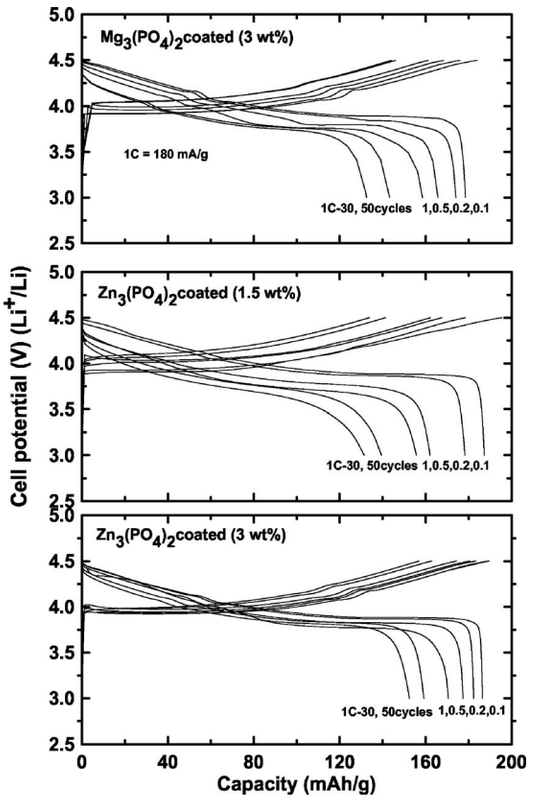

Figure 4. Plots of cycling curves of coin-type half cells containing uncoated and $Mg_3(PO_4)_2$ and $Zn_3(PO_4)_2$ nanoparticle-coated $LiCoO_2$ cathodes between 3 and 4.5 V at different C rates from 0.1 to 1C (1C = 180 mA/g) and after 30 and 50 cycles at a 1C rate. The same C rates were used during the charge and discharge processes. For the $Zn_3(PO_4)_2$ nanoparticle-coated $LiCoO_2$ cathodes, 1.5 and 3 wt % coating concentrations are compared.

samples (3 wt % coating) was 84 and 90%, respectively, after 50 cycles. The decreased capacity retention with the $Mg_3(PO_4)_2$ coating relative to $Zn_3(PO_4)_2$ coating occurred because the nonuniform coating layer with coated nanoparticles <50 nm in size impedes Li-ion diffusivity into the bulk particle. A similar result was observed in the $SrHPO_4$ and $CePO_4$-coated $LiNi_{0.9}Co_{0.1}O_2$ cathodes.[15] When the coating concentration of the $Zn_3(PO_4)_2$ coating decreases to 1.5 wt %, the first discharge capacity is slightly larger than that of the $Mg_3(PO_4)_2$ coating, at 187 mAh/g. However, the capacity retention at 1C rate cycling decreases to 140 mAh/g, which is comparable with that of $Mg_3(PO_4)_2$-coated $LiCoO_2$. Table II summarizes the capacities of the uncoated, coated, and doped cathodes at different rates and after 30 and 50 cycles of the samples. Overall, the coated samples demonstrate enhanced capacity retention at 1C rate cycling. It is believed that $M_3(PO_4)_2$ nanoparticles exist as an amorphous solid solution on the particle surface with a partial reaction of bulk $LiCoO_2$ during an annealing process at 800°C, which may enhance both Li-ion and electronic conductivities. However, in the case of the 1.5 wt % $Mg_3(PO_4)_2$-coated cathode consisting of both a thin coating layer ($\sim$2 nm) and abnormally large nanoparticles with size of $\sim$50 nm, these large nanoparticles may serve as absolute insulators, leading to decreased conductivities. The $Mg_3(PO_4)_2$-coated cathode (3 wt %) does not show such large particles on the surface and has a uniform coating thickness of $\sim$5 nm, although the reason for more a uniform coating layer formation than 1.5 wt % coating needs further investigation. The enhancement of electronic conductivities of the coated samples may be due to the formation of electronic holes in the solid solution near the particle surfaces, according to the reaction $2Co^{3+} \rightarrow 1Co^{4+} + M^{2+}$.[21,22] Based upon the above results, a more uniform coating is beneficial for both Li ion diffusivity and electronic conductivity. It is well

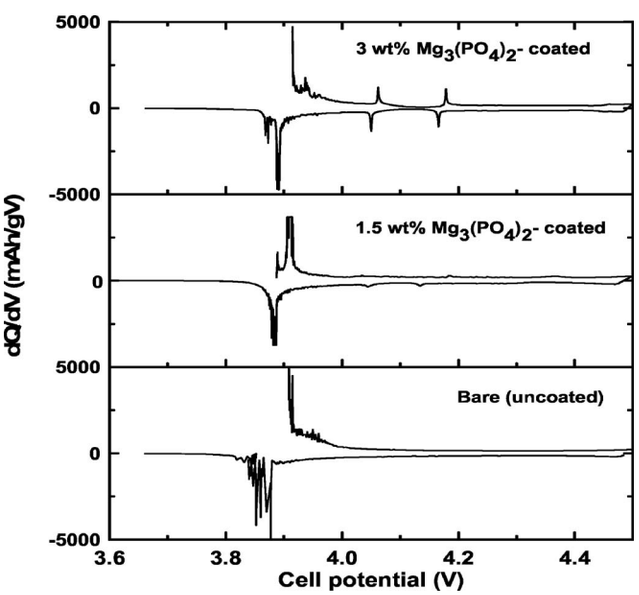

Figure 5. Differential voltage profiles for the uncoated 3, and 1.5 wt % $Mg_3(PO_4)_2$-coated cathodes in coin-type half cells.

Table II. Comparison of the first discharge capacities of $LiCo_{0.96}M_{0.04}O_2$ (M = Zn and Mg) and $Mg_3(PO_4)_2$ and $Zn_3(PO_4)_2$ nanoparticles-coated $LiCoO_2$ at 0.1, 0.2, 0.5, and 1C and at 1C after 30 and 50 cycles (1C = 180 mAh/g). Units are mAh/g.

Material	0.1C	0.2C	0.5C	1C	1C, 30 cycles	1C, 50 cycles
$LiCoO_2$	186	183	174	163	125	100
$LiCo_{0.96}Zn_{0.04}O_2$	175	164	151	139	79	
$LiCo_{0.96}Mg_{0.04}O_2$	175	169	155	141	79	
$Mg_3(PO_4)_2$ coating	179	174	166	159	143	133
$Zn_3(PO_4)_2$ coating (1.5 wt %)	187	178	162	156	140	131
$Zn_3(PO_4)_2$ coating (3 wt %)	187	182	176	171	159	153

known that large internal strains and subsequent mechanical degradation of the cathode materials originate from the dissolution of Li^+ and M^{4+} ions, and that the formation of by-products between reaction-dissolved ions and electrolytes at the interface enhances the structural degradation of the cathodes.[20,21] This effect becomes evident during storage at elevated temperatures.[16] A previous TEM result showed that an uncoated cathode charged at 4.5 V showed a structural transformation into the spinel phase at the particle surface after storage at 90°C for 4 h.[16,17]

Storage behavior of the cathode at 90°C, especially at the charged state, is different from that at room temperature due to accelerated reactions between the cathode surface and the electrolytes. Many Li-ion manufacturers have regarded the storage test at 90°C as the most severe test condition among the various test methods to verify the structure stability of the cathode. At this test condition, cathode material is believed to play a major role in swelling of the Li-ion cells. Accordingly, it is important to provide the storage results of the cathode materials such as XRD and dissolved metal contents. Figure 6 shows XRD patterns of the uncoated sample after charging to 4.5 V as well as that after 90°C storage at 1 day. After storage at 90°C for 1 day, peaks assigned to $Li_xCo_2O_4$, Co_3O_4 spinel phases, and CoO phases are observed; these had significantly increased in size. Moreover, unknown phases with strong intense peaks are observed, and the development of similar peaks was observed in the $Li_xNi_{0.86}Co_{0.1}Zn_{0.04}O_2$ cathode after storage at 90°C.[17] At a higher voltage, the Co^{4+} ions in the $LiCoO_2$ attack and oxidize the carbonate groups of the solvent molecules due to their acidic/nucleophilic properties and are reduced to Co^{2+}.[22] In addition, the formation of Co^{2+} simultaneously accompanies the formation of Li_2O, leading to a continuous increase of HF content, according to the reaction $Li_2O + H_2O \rightarrow 2LiOH + LiPF_6 \rightarrow 2HF + POF_3 + 2LiF$.[23] The H_2O source is the cathodes, and uncoated and coated cathodes had 120 and 80 ppm, respectively, as measured by a Karl–

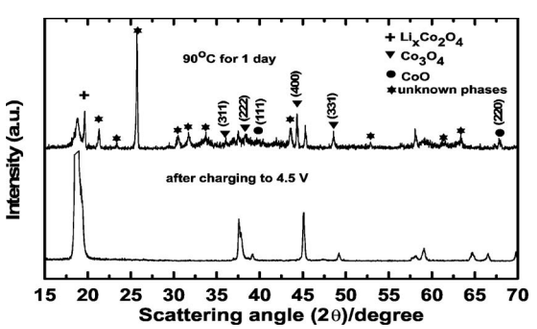

Figure 6. XRD patterns of a uncoated $LiCoO_2$ electrode after a 4.5 V charge and after storage at 90°C for 1 h. After charging the cell, the electrode was separated from the cell and kept in the electrolyte in a vial.

Table III. Amounts of the dissolved Co ions into the electrolytes and HF contents in $LiCo_{0.96}M_{0.04}O_2$ (M = Zn and Mg) and $Mg_3(PO_4)_2$ and $Zn_3(PO_4)_2$ nanoparticle-coated $LiCoO_2$ during storage at 90°C after 1 day after charging to 4.5 V vs lithium metal.

Material	Co	HF before storage (ppm)	HF after storage (ppm)
$LiCoO_2$	3000	200	900
$LiCo_{0.96}Zn_{0.04}O_2$	270	190	350
$LiCo_{0.96}Mg_{0.04}O_2$	900	210	500
$Zn_3(PO_4)_2$ coating (3 wt %)	70	90	30
$Mg_3(PO_4)_2$ coating	90	100	50

Fisher moisture titrator. Hence, it is important to blacken the Co^{4+} dissolution initially. In addition, the dissolved Li^+ ions are solvated and combine with Co^{4+}-oxidized solvent molecules to form lithium-containing organic products. As shown in Table III, the Co content in the uncoated sample after storage was 3500 ppm (before storage its amount was negligible). The HF content of the uncoated sample after storage increases to 800 ppm, compared to 200 ppm before storage. In consequence, the charged uncoated cathode undergoes severe structural instability at 90°C. The low-magnification TEM images of the uncoated cathode after storage at 90°C in Fig. 7a show the presence of rough surfaces and different contrasts near the surfaces, which indicates the presence of a highly defected phase. Essentially, the high-resolution image in Fig. 7b shows the formation of the amorphous phase that resulted from the severe dissolution of Li and Co at 90°C.

XRD patterns of the doped cathodes are, however, quite different from those of the uncoated cathode after storage at 90°C (Fig. 8). XRD patterns of the charged $LiCo_{0.96}Mg_{0.04}O_2$ electrode stored at 90°C show that the peak intensities of unknown phases are significantly decreased, although Co_3O_4 and CoO peaks continue to be present. For $LiCo_{0.96}Zn_{0.4}O_2$, unknown peaks including CoO and Co_3O_4 phases are not observed, except for a slightly increased peak-broadening effect, compared to that of the charged cathode. This result indicates that Zn or Mg doping into the $LiCoO_2$ causes an improvement in structural stability and reduces surface reactivity with the electrolyte, although Zn doping leads to a better result. This result is further supported by the amount of dissolved Co content in the electrolyte at 90°C. The Co contents of the Mg- and Zn-doped cathodes after storage were 900 and 270 ppm, respectively. Similarly, the HF content decreased in the doped cathodes; they were measured at 500 and 350 ppm, respectively, as shown in Table III. This result agrees with the XRD patterns of the doped cathodes kept at 90°C, as shown in Fig. 6. The TEM image (Fig. 9) of the $LiCo_{0.96}Mg_{0.04}O_2$ electrode shows the formation of the Co_3O_4 phase at the particle surface, while that of the $LiCo_{0.96}Zn_{0.04}O_2$ electrode shows a pristine layered phase.

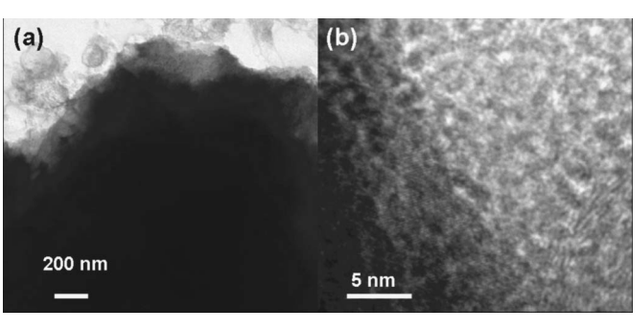

Figure 7. TEM images of uncoated electrodes after storage at 90°C for 1 day at 4.5 V.

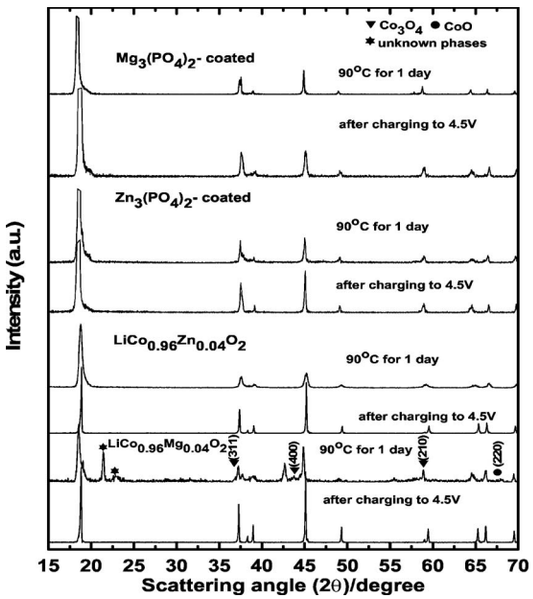

Figure 8. XRD patterns of the $LiCo_{0.96}M_{0.04}O_2$ (M = Zn and Mg) and $Mg_3(PO_4)_2$ and $Zn_3(PO_4)_2$ nanoparticle-coated $LiCoO_2$ electrodes after a 4.5 V charge and storage at 90°C for 1 h. After charging the cell, the electrode was separated from the cell and kept in the electrolyte in a vial.

As shown in Fig. 8, XRD patterns of the coated cathode after storage exhibit no peak spectral changes relative to those of the cathodes charged to 4.5 V, indicating that the surface coating layer effectively reduces the reactions with the electrolytes. It has been reported that the coating layers act as an HF scavenger.[24] As shown in Table III, the HF content after storage was significantly decreased to 30 and 50 ppm for the $Zn_3(PO_4)_2$ and $Mg_3(PO_4)_2$ coatings, respectively. This result is consistent with other studies that concluded that the surface coating layer gettered F^- ions from HF.[24-27] TEM images of the stored samples support the XRD spectral results in Fig. 8, and neither coated sample shows the formation of the spinel phase while maintaining the original layered phase. TEM images of both coated samples are similar to the Zn-doped cathode, with a coating layer that does not show damage. In contrast to the uncoated cathode, the TEM image of the $Mg_3(PO_4)_2$-coated cathode shows a smooth surface, which is indicative of the absence of a development of defect phases.

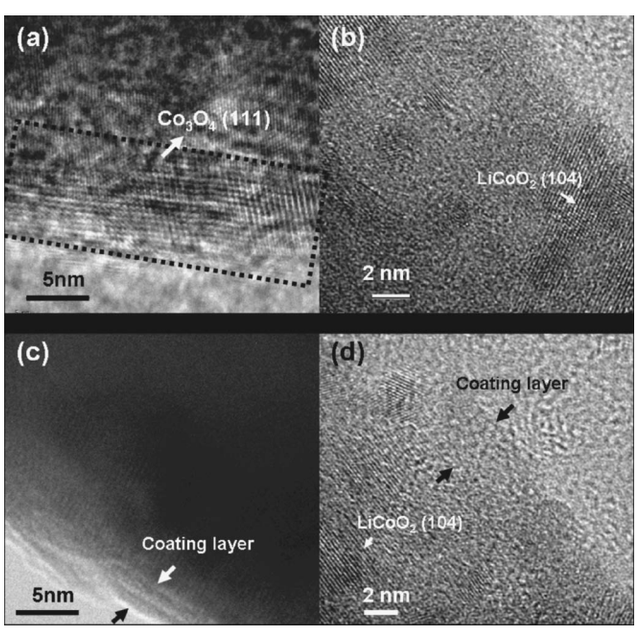

Figure 9. TEM images of (a) $LiCo_{0.96}Zn_{0.04}O_2$ and (b) $LiCo_{0.96}Zn_{0.04}O_2$ electrodes, after storage at 90°C for 1 day at 4.5 V and (c) $Mg_3(PO_4)_2$ and (d) $Zn_3(PO_4)_2$ nanoparticle-coated $LiCoO_2$ electrodes, after storage at 90°C for 1 day at 4.5 V.

Conclusions

In terms of electrochemical cycling and storage characteristics at 90°C, coated samples showed much-improved results relative to doped cathodes. In contrast to the doped cathodes, the coated samples were effective in retarding direct reactions between the electrolyte and the cathode surface that consisted of highly oxidized Co^{4+} ions. Overall, $Zn_3(PO_4)_2$-coated cathodes showed a first discharge capacity of 187 mAh/g and excellent capacity retention at 1C rate after 50 cycles, as shown by a 154 mAh/g measurement. This result indicates that the amorphous-like coating layer was effective for improving electrochemical activity and that it decreased side reactions with the electrolytes at 90°C as well.

Acknowledgments

This work was supported by Ministry of Information and Communication (MIC) and Institute for Information and Technology Advancement (IITA) through the Information Technology (IT) Leading Research and Development Support Project.

Kumoh National Institute of Technology assisted in meeting the publication cost of this article.

References

1. M. Zou, M. Yoshio, S. Gopukumar, and J.-I. Yamaki, *Chem. Mater.*, **15**, 4699 (2003).
2. Y.-I. Jang, B. Haung, H. Wang, D. R. Sadoway, G. Ceder, Y.-M. Chiang, H. Liu, and H. Tamura, *J. Electrochem. Soc.*, **146**, 862 (1999).
3. J. Cho, Y. J. Kim, T.-J. Kim, and B. Park, *Angew. Chem., Int. Ed.*, **40**, 3367 (2001).
4. J. Cho, Y. J. Kim, and B. Park, *Chem. Mater.*, **12**, 3788 (2000).
5. J. Cho, J.-G. Lee, B. Kim, and B. Park, *Chem. Mater.*, **15**, 3190 (2003).
6. J. Cho, Y.-W. Kim, B. Kim, J.-G. Lee, and B. Park, *Angew. Chem., Int. Ed.*, **42**, 1618 (2003).
7. J. Cho, *J. Power Sources*, **126**, 186 (2004).
8. J. Cho, *Electrochim. Acta*, **48**, 2807 (2003).
9. J. Cho, *Electrochem. Commun.*, **5**, 146 (2003).
10. Z. Zhang, Z. Gong, and Y. Yang, *J. Phys. Chem. B*, **108**, 17546 (2004).
11. Y. Jin, N. Li, C. H. Chen, and S. Q. Wei, *Electrochem. Solid-State Lett.*, **9**, A273 (2006).
12. G. V. S. Rao, B. V. R. Chowdari, and H. J. Linder, *J. Power Sources*, **97-98**, 313 (2001).
13. Y. Bai, N. Liu, J. Liu, Z. Wang, and L. Chen, *Electrochem. Solid-State Lett.*, **9**, A552 (2006).
14. Y.-K. Sun, S.-W. Cho, S.-W. Lee, C. S. Yoon, and K. Amine, *J. Electrochem. Soc.*, **154**, A168 (2007).
15. H. Lee, Y. Kim, Y.-S. Hong, Y. Kim, M. G. Kim, N.-S. Shin, and J. Cho, *J. Electrochem. Soc.*, **153**, A781 (2006).
16. H. Lee, M. G. Kim, and J. Cho, *Electrochem. Commun.*, **9**, 149 (2007).
17. Y. Kim and J. Cho, *J. Electrochem. Soc.*, **154**, A495 (2007).
18. J. N. Reimers and J. R. Dahn, *J. Electrochem. Soc.*, **139**, 2091 (1992).
19. J.-G. Lee, B. Kim, J. Cho, Y.-W. Kim, and B. Park, *J. Electrochem. Soc.*, **151**, A801 (2004).
20. N. Pereira, C. Matthias, K. Bell, F. Badway, I. Plitz, J. Al-Sharab, F. Cosandey, P. Shah, N. Isaacs, and G. G. Amatucci, *J. Electrochem. Soc.*, **152**, A114 (2005).
21. H. Tukamoto and A. R. West, *J. Electrochem. Soc.*, **144**, 3164 (1997).
22. S. Lavasseur, M. Menetrier, and C. Delmas, *Chem. Mater.*, **14**, 3584 (2002).
23. Y.-I. Jang, N. J. Dudney, D. A. Blom, and L. F. Allard, *J. Electrochem. Soc.*, **149**, A1442 (2002).
24. G. G. Amatucci, J. M. Tarascon, and L. C. Klein, *Solid State Ionics*, **83**, 167 (1996).
25. Z. Wang and L. Chen, *J. Power Sources*, **146**, 254 (2005).
26. B. Markovsky, A. Rodkin, G. Salitra, Y. Talyosef, D. Aurbach, and H.-J. Kim, *J. Electrochem. Soc.*, **151**, A1068 (2004).
27. J.-S. Kim, C. S. Johnson, J. T. Vaughey, S. A. Hackney, K. A. Walz, W. A. Zeltner, M. A. Anderson, and M. M. Thackeray, *J. Electrochem. Soc.*, **151**, A1755 (2004).